Materials Chemistry and Physics 321 (2024) 129503

Contents lists available at ScienceDirect

Materials Chemistry and Physics

journal homepage: www.elsevier.com/locate/matchemphys

Investigating long term storage stability and drug release behavior of polypeptide based fibrous scaffold for tissue engineering application

Chun-Yu Chang [a,c], An-Jey A. Su [b], Meng-Fang Lin [c], Kai-Chi Hsiao [d], Chia-Hsien Lee [c], Yu-Ting Lin [c,e], Yu-Sheng Hsiao [e], Ming-Chung Wu [d,**], Yu-Ching Huang [c,***], Wei-Fang Su [c,f,*]

[a] Bachelor Program in Semiconductor Materials and Fabrication, Ming Chi University of Technology, Taiwan
[b] Dept. of Surgery, Anschutz Medical Campus, University of Colorado, Aurora, CO, USA
[c] Dept. of Materials Engineering, Ming Chi University of Technology, Taiwan
[d] Dept. of Chemical and Materials Engineering, Chang Gung University, Taiwan
[e] Dept. of Materials Science and Engineering, National Taiwan University of Science and Technology, Taipei City, Taiwan
[f] Dept. of Materials Science and Engineering, National Taiwan University, Taiwan

HIGHLIGHTS

- A systematically investigated storage stability and drug release behavior of polypeptide-based fibrous scaffold.
- Gravity impact on PBG scaffold felt storage led to an increase in fiber diameter on the bottom side of the scaffold.
- The tensile strength of both PBG and PBGMH4 scaffolds increases as the storage time increases.
- PBGMH4 scaffolds exhibit superior storage stability due electrostatic repulsion from MH.
- The specific surface area of the scaffold plays a critical role in controlling drug release kinetics.

GRAPHICAL ABSTRACT

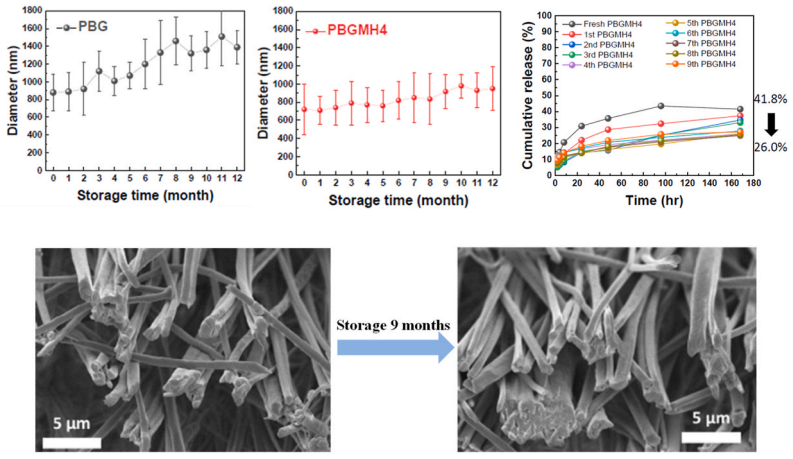

ARTICLE INFO

Keywords:
Electrospinning
Scaffold
Drug delivery
Polypeptide
Storage stability

ABSTRACT

Electrospun poly (γ-benzyl-L-glutamate) (PBG) scaffold felt with aligned fibers shows promising nerve regeneration and neurite growth capability due to the nerve stimulating moiety of glutamate in the PBG material. The nerve regeneration capability can be further enhanced by incorporating 4 wt% minocycline hydrochloride (MH) in the scaffold (PBGMH4). They are useful in the nerve tissue engineering to repair and regeneration damaged nerves in central nerve system or peripheral nerve system. Here we investigate the ambient storage capability of PBG and PBGMH4 by monitoring the changes over time of fiber dimension, mechanical properties of both

* Corresponding author. Dept. of Materials Engineering, Ming Chi University of Technology, Taiwan.
** Corresponding author.
*** Corresponding author.
E-mail addresses: mingchungwu@mail.cgu.edu.tw (M.-C. Wu), huangyc@mail.mcut.edu.tw (Y.-C. Huang), suwf@ntu.edu.tw (W.-F. Su).

https://doi.org/10.1016/j.matchemphys.2024.129503
Received 21 March 2024; Received in revised form 18 May 2024; Accepted 21 May 2024
Available online 23 May 2024

scaffolds and amount of drug release of PBGMH4. It is interesting to observe the diameter of fibers and mechanical strength of scaffolds increases but the amount of drug release decrease with time. By carefully examining the top view of the scaffolds using scanning electron microscopy (SEM), the fiber diameter of PBG increased by 58 % over the 12 months storage period, which is larger than the 32 % increase observed for PBGMH4. Furthermore, after storage for 12 months, the difference in fiber diameter between the top and bottom sides of PBG scaffold is 25.9 %, whereas for PBGMH4 is only 6.3 %. These results demonstrate that the PBGMH4 scaffold exhibits superior storage stability compared to that of PBG. Because the fibers of the scaffolds are aligned without any crosslinkage, the scaffolds are porous structure of felts. The porosity of PBGMH4 scaffold is decreased from 90 % to 72 % which can be accountable for the decrease of drug release from initial 42 % to a stabilized 26 % after 9 months of storage. The results indicate the specific surface area of the scaffolds play an important role in governing drug release kinetics. This study thoroughly investigates the storage stability of PBG and PBGMH4 electrospun fibrous scaffolds. The observed correlations between fiber diameter, mechanical properties, and drug release behavior hold implications for the design of advanced bioscaffolds. The long shelf life of optimal PBGMH4 scaffold shows potential application for the nerve regeneration and controlled drug delivery systems.

1. Introduction

Neural tissue engineering is recognized as a highly promising field to offer innovative solutions for treating various neurological diseases, including both central nervous system and peripheral nervous system pathologies [1–3]. Neural cells are initially cultivated on biomimetic scaffolds in vitro before being transplanted to damaged neural sites for repair and regeneration. These scaffolds play a crucial role as a supportive framework, facilitating cell growth, differentiation, and repair to aid in the restoration the function of damaged tissues [4–6]. Selecting the appropriate scaffold material is crucial for achieving optimal nerve regeneration [7–9].

Polypeptides are biomimetic polymers extensively employed in biomedical applications due to their excellent biocompatibility and biodegradability [10–14]. Different types of amino acids enable these polymers to possess specific functionalities [15–19]. Poly(γ-benzyl-L-glutamate) (PBG) is a kind of polypeptide that comprises L-glutamate, known as a crucial neurotransmitter that stimulates nerve growth [20–22]. Additionally, the monomer of PBG contains a benzyl ester group to protect the COOH of glutamic acid side chain from undesired reaction during monomer synthesis and polymerization, resulting in PBG having a regular linear main chain with steady chemical properties [23–26]. The PBG can be used to fabricate fibrous scaffolds through the electrospinning process. The fibrous scaffolds have various applications such as mimicking the extracellular matrix or precise delivering drugs to promote nerve regeneration [27–31]. Scaffold fabricate from PBG can reduce the risk of immune and rejection reaction between the material and nerve cells. Our previous research results have shown that PBG scaffolds exhibit good in vitro [32] and in vivo [33] biocompatibility with slow biodegradation [34], making PBG an ideal choice for treating neurological diseases. On the other hand, in tissue engineering, a neuroprotective antibiotic drug called minocycline hydrochloride (MH) has been proven to have beneficial effects in promoting the proliferation and growth of neural cells [35–37]. However, the half-life of MH in vivo is quite short, necessitating scientist to find suitable scaffolds to support MH for sustained drug delivery. Previous studies have found that PBG fibrous scaffold incorporate with 4 wt% of MH (PBGMH4) can release MH steadily, further enhancing its application value in neural tissue engineering [38].

Although PBG fibrous scaffolds combined with MH drugs effectively assist in neural differentiation and growth, considerations for successfully applying these scaffold materials in clinical practice need to extend beyond their biocompatibility and functionality to include their stability during long-term storage in the ambient environment. Therefore, in this study, we conduct a comprehensive experiment of PBG and PBGMH4 scaffolds over a storage period of up to 12 months. We explore various parameters including changes in fiber diameter, mechanical properties, porosity, and the capability to release MH over time. Through these detailed investigations, we aim to gain deeper insights into the performance characteristics of these scaffold materials. This knowledge will provide a more robust foundation for future clinical applications, ensuring the safety, effectiveness, and long-term stability in healthcare settings.

2. Results and discussion

The chemical structures of PBG and MH are shown in Fig. S1. In order to investigate the storage stability of PBG and PBGMH4 aligned fiber scaffolds felts, we prepared them via electrospinning and subsequently stored them under ambient conditions of 25 ± 1 °C and 50 ± 5 %RH. We monitored the variation in fiber diameter on the top side of the felts over a storage period of 12 months, as shown in Fig. 1, and summarized the diameter data in Table S1. Detailed SEM top view images of the fiber scaffolds for each month are available in Fig. S2. The initial fiber diameters of PBG and PBGMH4 scaffold were 880 nm and 720 nm, respectively. The smaller size of the PBGMH4 fiber diameter can be attributed to the presence of MH, which acts as a salt. MH enhances the conductivity of the PBG solution and facilitates easier fiber formation

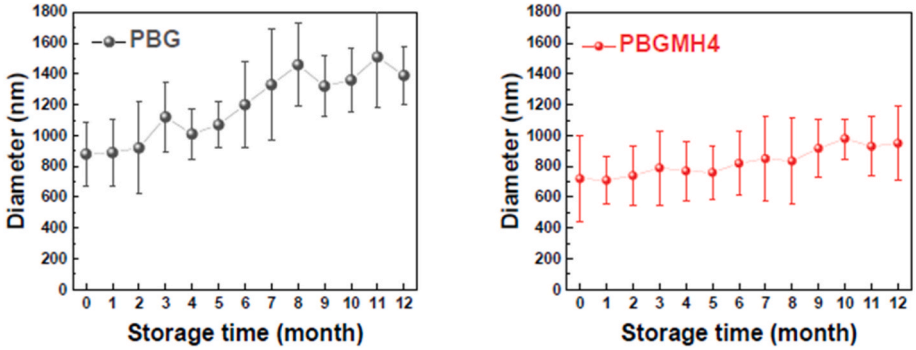

Fig. 1. Top side fiber diameter variation in PBG and PBGMH4 scaffold felts over a storage period of 12 months.

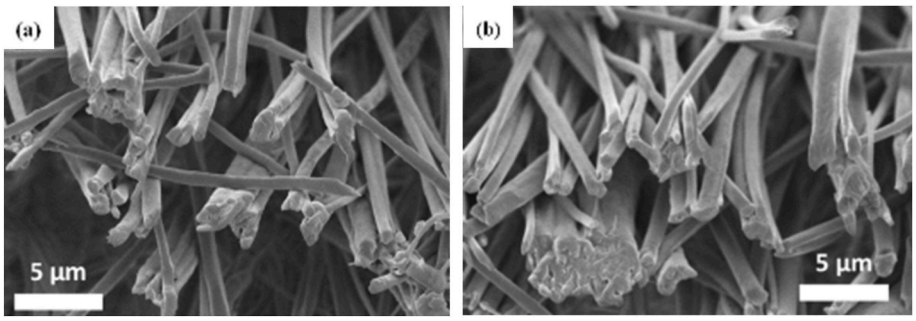

Fig. 2. SEM cross-section images of PBG scaffolds felts (a) just prepared by electrospinning and (b) after 9 months of storage.

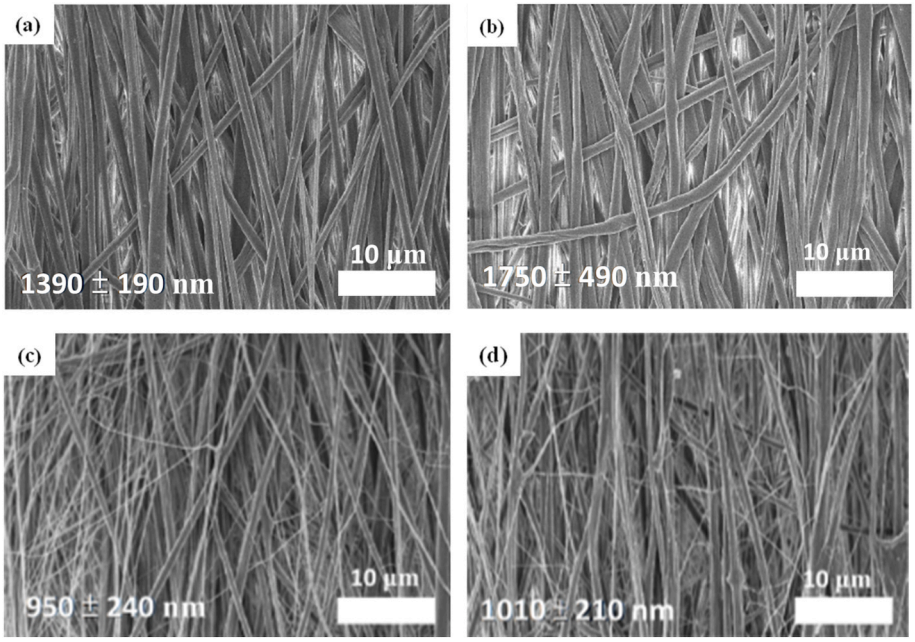

Fig. 3. SEM images of the top and bottom sides of PBG scaffold felts after 12 months of storage are presented in (a) and (b) respectively, while corresponding images of PBGMH4 scaffold felts following the same duration of storage are shown in (c) and (d).

during the initial high-voltage electrospinning process. This charge effect leads to a size difference of 22.2 % [=(880-720)/720] between PBG and PBGMH4 scaffolds.

As the storage time increases, the fiber diameter of the PBG scaffold evidently increases. Under 25 ± 1 °C and 50 ± 5 %RH storage conditions, the fiber diameter of PBG increased by 58 % [=(1390-880)/880] over the 12 months storage period. On the other hand, the fiber diameter of PBGMH4 scaffold increases slowly, with only a 32 % [=(950-720)/720] increase after 12 months of storage. The main reason for the difference in fiber diameter increment is that with prolonged storage time, the weak van der Waals forces between PBG polymer chains gradually cause them to merge. In contrast, the presence of MH in the PBGMH4 scaffold, along with minocycline carrying NH_3^+ functional groups, leads to electrostatic repulsion between fibers and therefore prevents them from merging. This demonstrates that the PBGMH4 scaffold exhibits superior storage stability compared to that of PBG.

As a result of extended storage, the fiber diameter on the top side of PBG scaffold felt has significantly increased. Consequently, we compared the SEM cross-section images of freshly prepared PBG scaffolds with those that have undergone long-term storage, to observe whether there are changes in fiber diameter in the vertical direction of the scaffold felt. The SEM cross-section images are shown in Fig. 2. Analysis of these images reveals that the freshly prepared PBG scaffold has fine fiber diameter with minimal merging. However, after 9 months of storage, fibers are noticeably merging together. This is because, in addition to van der Waals forces, the gravity effect on each fiber also cause them to approach each other and sink downwards, ultimately leading to the merge of fibers in the PBG scaffold.

To verify the impact of gravity on the storage stability of scaffold felt, we also compared the top and bottom side SEM images of PBG and PBGMH4 scaffold felt, as shown in Fig. 3. Observation of samples stored for 12 months reveals a significant variance in fiber diameter between the top and bottom sides of PBG scaffold felt, with a difference of 25.9 % [=(1750-1390)/1390]. This indicates that beyond van der Waals forces, PBG scaffold felt is also influenced by gravity, causing fibers to merge together and resulting in thicker fibers on the bottom side compared to the top side. On the other hand, PBGMH4 scaffold felt shows only a 6.3 % [=(1010-950)/950] difference in fiber diameter between the top and bottom sides. This suggests that while fibers in PBGMH4 scaffold felt are also affected by gravity and tend to merge, the electrostatic repulsion partially counteracts the effect of gravity, thus further demonstrating that PBGMH4 scaffold felt has better storage stability compared to PBG ones.

In the field of neural tissue engineering, the mechanical strength of scaffolds plays a significant role in cell proliferation and growth. Therefore, the variation of scaffold mechanical strength with storage time is a crucial issue when investigating scaffold stability. It has been observed that the diameter of fibers increases with storage time,

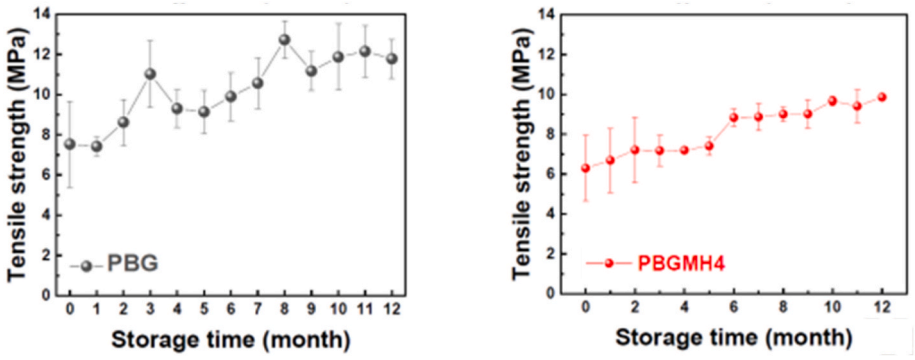

Fig. 4. Maximum tensile strength variation of PBG and PBGMH4 scaffold felts over a storage period of 12 months.

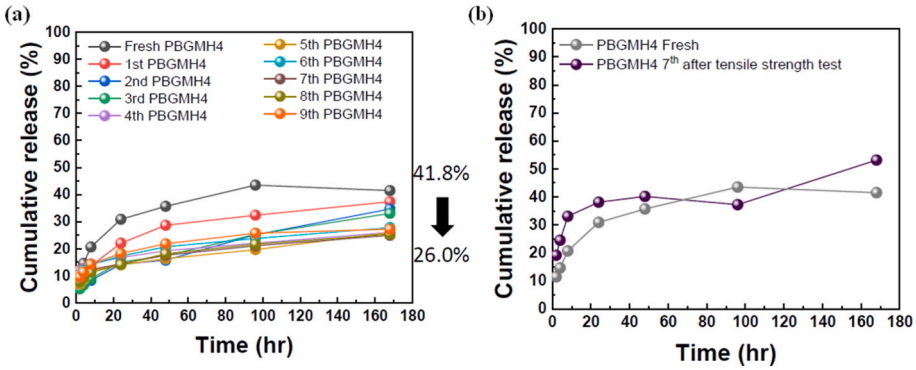

Fig. 5. (a) Cumulative drug release profiles of PBGMH4 scaffolds with various storage times. (b) Cumulative drug release profiles of PBGMH4 fresh electrospun scaffolds and storage 7 months after tensile strength test.

indicating an expected change in the mechanical properties of scaffold felts. The variation of maximum tensile strength over storage time for PBG and PBGMH4 scaffold felts is shown in Fig. 4 and summarized in Table S2. The initial maximum tensile strengths of PBG and PBGMH4 scaffold felts are 7.53 MPa and 6.30 MPa, respectively. The slightly lower maximum tensile strength of PBGMH4 scaffold felts compared to PBG ones is reasonable, given the smaller initial fiber diameter of PBGMH4 scaffold felts. With increasing storage time, both PBG and PBGMH4 scaffold felts exhibit a gradual increase in maximum tensile strength, consistent with the increase in fiber diameter. Ultimately, the maximum tensile strengths of PBG and PBGMH4 scaffold felts reach 11.78 MPa and 9.86 MPa, respectively.

The cumulative drug release profiles of PBGMH4 scaffolds with various storage times are depicted in Fig. 5(a). PBGMH4 scaffold felts were stored under ambient conditions of 25 ± 1 °C and 50 ± 5 %RH, with one sample taken out every month for a 7 days drug release test. The experimental results demonstrate that PBGMH4 scaffold can slowly and steadily release MH, indicating it as an excellent drug release carrier. However, despite the increase in fiber diameter and mechanical properties with storage time, the amount of cumulative drug release after 7 days gradually decreases. The freshly prepared PBGMH4 scaffold felt exhibits a cumulative drug release of 41.8 % over 7 days, but after 9 months of storage, the cumulative drug release decreases to 26.0 %. We speculate that since the fibers of both PBG and PBGMH4 scaffold are aligned without any crosslinks, they form a porous felt structure. With prolonged storage, fiber merging leads to an increase in diameter, resulting in a decrease in the porosity of PBGMH4 scaffold felt from 90 % to 72 % as measured by mercury porosimetry. This reduction in porosity decreases the specific surface area of PBGMH4 scaffold, consequently lowering its drug release capacity.

To verify if the decrease in specific surface area causes the decline in drug release capacity, we randomly selected a PBGMH4 scaffold stored for an extended period and conducted a drug release test after undergoing tensile testing (in this case, a sample stored for 7 months), as shown in Fig. 5(b). Since above results indicate that the fiber merging is due to physical factors including gravity and van der Waals forces rather than forming chemical bond, the merged fibers were pulled apart after tensile testing and increasing the specific surface area again. Consequently, the drug release capacity is restored to a level similar to that of the freshly prepared PBGMH4 scaffold felt. These results emphasize the crucial role of scaffold specific surface area in governing drug release kinetics. To overcome the problem of fiber merging and subsequent reduction in porosity leading to decreased drug release capacity over time, future research could focus on incorporating surface modification techniques into the scaffold fabrication process. Surface modifications such as crosslinking or introducing charged functional groups could potentially reduce the effects of van der Waals forces and gravity, thereby maintaining scaffold integrity over extended periods.

3. Conclusions

Through long term monitoring and analysis of the storage stability of PBG and PBGMH4 fiber scaffold felts, we have discovered that PBGMH4 exhibits superior stability during storage. This is attributed to the presence of MH in PBGMH4, which induce electrostatic repulsion between fibers and thus preventing their merging. In contrast, PBG fiber scaffold felts showed a significant increase in fiber diameter during storage, causing the fibers within the scaffolds to settle down due to gravity. We have observed the increase in fiber diameter leads to an increase in the maximum tensile strength of the scaffold. PBGMH4 scaffold show promising potential as drug release carriers due to the slowly and steadily release of MH. However, the drug release capacity decreased over time due to reduced specific surface area caused from fiber merging. Nevertheless, our study indicates that the drug release

capacity can be restored by physically pulling apart merged fibers after tensile testing, emphasizing the crucial role of scaffold specific surface area in controlling drug release kinetics. Our research reveals that PBGMH4 scaffold felts possess excellent storage stability and drug release performance, providing important insights and guidance for further research and applications in the field of neural tissue engineering.

4. Materials and methods

4.1. Materials

The experimental chemicals used in this study are listed as following: L-glutamate γ-benzyl ester (99 %, molecular weight = 237.30 g/mol, Sigma-Aldrich), propylene oxide (95 %, Acros), triphosgene (98 %, Sigma-Aldrich), sodium (99 %, Sigma-Aldrich), tetrahydrofuran (99.8 %, Honeywell), N,N-dimethylacetamide (DMAc, 99+%, Acros), methanol (99.8 %, extra dry over molecular sieve, Thermo Scientic) and minocycline hydrochloride (MH, 98.0 %, TCI). Anhydrous solvents of ethyl acetate (EA, ≥99.5 %, Macron Fine Chemicals) and benzene (99.7 %, Sigma) were prepared by dehydrating purchased solvents using 4A molecular sieves (4–8 mesh; Acros) and overnight nitrogen purging.

4.2. Synthesis of monomer and polymer

The monomeric and polymeric materials were synthesized according to the previous report [30] and illustrate below in brief.

4.2.1. Synthesis of monomer (γ-benzyl-L-glutamate N-carboxyanhydride, BGNCA)

6 g of L-glutamate γ-benzyl ester, 90 mL of anhydrous THF, and 7.8 ml of propylene oxide were added and stirred in a three necks round bottom flask for 5 min. Then 3.7g of triphosgene was added, and the solution was stirred for 2 h at room temperature until clear. The solution was concentrated using a rotary evaporator at 30 °C in order to remove byproducts. Subsequently, 60 ml of anhydrous THF was added, and then n-hexane was added dropwise until precipitation occurred. After overnight crystallization at -20 °C, the solution was filtered to collect the precipitation. This recrystallization procedure was repeated three times and the crystals were dried in a vacuum oven at 40 °C. A yield of 82 % BGNCA was obtained with a molecular weight of 263.25 g/mol.

4.2.2. Synthesis of polymer (poly(γ-benzyl-L-glutamate), PBG))

All three-neck flasks used for polymerization need to be vacuumed overnight to remove moisture before used. Add 3 g of BGNCA into the 100 ml flask and perform three cycles of vacuum and nitrogen purge. Afterward, inject 300 ml of dry benzene to disperse BGNCA. For the polymerization, sodium methoxide was used as the initiator, which was prepared by dissolving 75 mg of sodium in 10 ml of benzene and 5 ml of anhydrous methanol. Initiate polymerization by adding 0.344 ml of sodium methoxide into as-prepared BGNCA solution. After reacting at room temperature for 48 h in nitrogen atmosphere, the resulting polymer solution was precipitated and filtrated from ethyl acetate, followed by drying in a vacuum oven at 40 °C overnight. A yield of 91 % PBG was obtained with Mw = 631 kDa, Mn = 528 kDa and PDI = 1.19.

4.3. Scaffold fabrication

4.3.1. Preparation of PBG and PBGMH4 solution for electrospinning

The PBG solution for electrospinning was prepared by dissolving PBG in a co-solvent of THF and DMAc (7:3 v/v) overnight to achieve a concentration of 15 wt%. Similarly, the PBGMH4 solution was prepared by incorporating 4 wt% of MH (relate to the amount of PBG) to the same co-solvent of THF and DMAc (7:3 v/v) overnight, and also reaching a solution concentration of 15 wt%.

4.3.2. Electrospinning of PBG and PBGMH4

The electrospinning scaffolds were prepared under ambient conditions of 25 ± 1 °C and 50 ± 5 %RH. The setup involved placing a grounded rotating collector at a distance of 10 cm from the needle tip. An applied voltage of 20 kV and a flow rate of 5 ml/h were employed. The collector was enveloped in aluminum foil and rotated at a speed of 1500 rpm, while fibers were collected on it over a span of around 30 min. The final thickness of the resultant felt was within the range of 30–50 μm controlled by adjusting the collection time. The stability test was conducted by electrospinning one batch of PBG and PBGMH4 solution at one time. Subsequently, the electrospinning scaffold was divided into 12 pieces. The fibrous scaffolds are stored at 25 ± 1 °C and 50 ± 5 %RH for the 12 months stability experiments. One piece of scaffold was taken out for examination each month.

4.4. Characterization

4.4.1. Characterization of electrospinning scaffolds

The fiber diameter and the cross-section images of PBG and PBGMH4 scaffold was measured by SEM (SU-8010, Hitachi). The porosity of scaffold felt was determined by mercury porosimetry (micromeritics AutoPore IV 9520). The mechanical properties of the scaffold felts were measured by the tensile test machine (YH–H31B7, Yang Yi Technology). The sample size for tensile strength test was 2 cm in width and 15 cm in length.

4.4.2. Drug release

The UV–vis absorption spectrometer (UV-1900, Shimadzu) was used to establish calibration curves (as shown in Fig. S3) at wavelength 245 nm of MH in phosphate buffered saline solution (PBS) solution to estimate the cumulative drug release of PBGMH4. The electrospinning scaffold samples were cut into 2 cm × 2 cm in pieces and immersed in PBS solution. The cumulative release of drug over a specific storage month can be calculated by following equation [30]:

$$\text{cumulative release}(\%) = \frac{M_t}{M_\infty} \times 100\%$$

where M_t stands for the cumulative amount of drug release at time t and M_∞ denotes the total amount of MH drug.

CRediT authorship contribution statement

Chun-Yu Chang: Writing – review & editing, Writing – original draft, Methodology. **An-Jey A. Su:** Methodology, Investigation. **Meng-Fang Lin:** Resources. **Kai-Chi Hsiao:** Validation, Investigation. **Chia-Hsien Lee:** Investigation. **Yu-Ting Lin:** Investigation. **Yu-Sheng Hsiao:** Resources. **Ming-Chung Wu:** Resources, Project administration. **Yu-Ching Huang:** Resources, Project administration, Funding acquisition. **Wei-Fang Su:** Writing – review & editing, Supervision, Conceptualization.

Declaration of competing interest

The authors declare that they have no known competing financial interests or personal relationships that could have appeared to influence the work reported in this paper.

Data availability

No data was used for the research described in the article.

Acknowledgment

The authors highly appreciated the financial support obtained from National Science and Technology Council of Taiwan in this research

(NSTC 113-2222-E-131-001, NSTC 112-2622-E-131-001, NSTC 112-2628-E-131-001-MY4 and NSTC 111-2221-E-131-019-MY3).

Appendix A. Supplementary data

Supplementary data to this article can be found online at https://doi.org/10.1016/j.matchemphys.2024.129503.

References

[1] C. Simitzi, A. Ranella, E. Stratakis, Controlling the morphology and outgrowth of nerve and neuroglial cells: the effect of surface topography, Acta Biomater. 51 (2017) 21–52.

[2] M.E. Gomes, M.T. Rodrigues, R.M. Domingues, R.L. Reis, Tissue engineering and regenerative medicine: new trends and directions-a year in review, Tissue Eng. B Rev. 23 (2017) 211–224.

[3] J. Wu, C. Hu, Z. Tang, Q. Yu, X. Liu, H. Chen, Tissue-engineered vascular grafts: balance of the four major requirements, Colloid Interface Sci. Commun. 23 (2018) 34–44.

[4] W. Xue, W. Shi, Y. Kong, M. Kuss, B. Duan, Anisotropic scaffolds for peripheral nerve and spinal cord regeneration, Bioact. Mater. 6 (2021) 4141–4160.

[5] J. Du, H. Chen, L. Qing, X. Yang, X. Jia, Biomimetic neural scaffolds: a crucial step towards optimal peripheral nerve regeneration, Biomater. Sci. 6 (2018) 1299–1311.

[6] S. Yi, L. Xu, X. Gu, Scaffolds for peripheral nerve repair and reconstruction, Exp. Neurol. 319 (2019) 112761.

[7] R. Boni, A. Ali, A. Shavandi, A.N. Clarkson, Current and novel polymeric biomaterials for neural tissue engineering, J. Biomed. Sci. 25 (2018) 1–21.

[8] Y. Qian, H. Lin, Z. Yan, J. Shi, C. Fan, Functional nanomaterials in peripheral nerve regeneration: scaffold design, chemical principles and microenvironmental remodeling, Mater. Today 51 (2021) 165–187.

[9] A.C. Pinho, A.C. Fonseca, A.C. Serra, J.D. Santos, J.F.J. Coelho, Peripheral nerve regeneration: current status and new strategies using polymeric materials, Adv. Healthcare Mater. 5 (2016) 2732–2744.

[10] R. Bucci, E. Georgilis, A.M. Bittner, M.L. Gelmi, F. Clerici, Peptide-based electrospun fibers: current status and emerging developments, Nanomaterials 11 (2021) 1262.

[11] H. Yoshida, D. Klee, M. Möller, M. Akashi, Creation of superhydrophobic electrospun nonwovens fabricated from naturally occurring poly(amino acid) derivatives, Adv. Funct. Mater. 24 (2014) 6359–6364.

[12] K. Klimek, G. Ginalska, Proteins and peptides as important modifiers of the polymer scaffolds for tissue engineering applications—a review, Polymers 12 (2020) 844.

[13] A. Song, A.A. Rane, K.L. Christman, Antibacterial and cell-adhesive polypeptide and poly(ethylene glycol) hydrogel as a potential scaffold for wound healing, Acta Biomater. 8 (2012) 41–50.

[14] K. Hosoyama, C. Lazurko, M. Muñoz, C.D. McTiernan, E.I. Alarcon, Peptide-based functional biomaterials for soft-tissue repair, Front. Bioeng. Biotechnol. 7 (2019) 205.

[15] T.L. Ma, C.M. Tsai, S.C. Luo, W.L. Chen, Y.C. Huang, W.F. Su, Chemical structures and compositions of peptide copolymer films affect their functional properties for cell adhesion and cell viability, React. Funct. Polym. 175 (2022) 105265.

[16] H.K. Kordasht, M. Hasanzadeh, F. Seidi, P.M. Alizadeh, Poly (amino acids) towards sensing: recent progress and challenges, Trac.Trend Anal. Chem. 140 (2021) 116279.

[17] M. Thompson, C. Scholz, Highly branched polymers based on poly(amino acid)s for biomedical application, Nanomaterials 11 (2021) 1119.

[18] T.Y. Yu, Y.H. Tseng, C.C. Wang, T.H. Lin, M.C. Wu, C.S. Tsao, W.F. Su, Three-level hierarchical 3D network formation and structure elucidation of wet hydrogel of tunable-high-strength nanocomposites, Macromol. Mater. Eng. 307 (2022) 2100871.

[19] Y. Ji, W. Song, L. Xu, D.G. Yu, S.W.A. Bligh, A review on electrospun poly(amino acid) nanofibers and their applications of hemostasis and wound healing, Biomolecules 12 (2022) 794.

[20] Y. Zhou, N.C. Danbolt, Glutamate as a neurotransmitter in the healthy brain, J. Neural. Transm. 121 (2014) 799–817.

[21] M.J. Niciu, B. Kelmendi, G. Sanacora, Overview of glutamatergic neurotransmission in the nervous system, Pharmacol. Biochem. Behav. 100 (2012) 656–664.

[22] S.R. Platt, The role of glutamate in central nervous system health and disease – a review, Vet. J. 173 (2007) 278–286.

[23] P. Papadopoulos, G. Floudas, H.-A. Klok, I. Schnell, T. Pakula, Self-assembly and dynamics of poly(γ-benzyl-l-glutamate) peptides, Biomacromolecules 5 (2004) 81–91.

[24] J.D. Han, J.X. Ding, Z.C. Wang, S.F. Yan, X.L. Zhuang, X.S. Chen, J.B. Yin, The synthesis, deprotection and properties of poly(γ-benzyl-L-glutamate), Sci. China Chem. 56 (2013) 729–738.

[25] H. Cao, J. Yao, Z. Shao, Synthesis of poly (γ-benzyl-L-glutamate) with well-defined terminal structures and its block polypeptides with alanine, leucine and phenylalanine, Polym. Int. 61 (2012) 774–779.

[26] A. Marx, C. Thiele, Orientational properties of poly-γ-benzyl-L-glutamate: influence of molecular weight and solvent on order parameters of the solute, Chem. Eur J. 15 (2009) 254–260.

[27] M. Khoroushi, M.R. Foroughi, S. Karbasi, B. Hashemibeni, A.A. Khademi, Effect of polyhydroxybutyrate/chitosan/bioglass nanofiber scaffold on proliferation and differentiation of stem cells from human exfoliated deciduous teeth into odontoblast-like cells, Mater. Sci. Eng. C 89 (2018) 128–139.

[28] S. Razavi, H. Zarkesh-Esfahani, M. Morshed, S. Vaezifar, S. Karbasi, M.A. Golozar, Nanobiocomposite of poly(lactide-co-glycolide)/chitosan electrospun scaffold can promote proliferation and transdifferentiation of Schwann-like cells from human adipose-derived stem cells, J. Biomed. Mater. Res. 103A (2015) 2628–2634.

[29] A.H. Tehrani, A. Zadhoush, S. Karbasi, H. Sadeghi-Aliabadi, Scaffold percolative efficiency: in vitro evaluation of the structural criterion for electrospun mats, J. Mater. Sci. Mater. Med. 21 (2010) 2989–2998.

[30] A.K. Tar, S. Karbasi, E. Naghashzargar, H. Salehi, Biodegradation and cellular evaluation of aligned and random poly (3-hydroxybutyrate)/chitosan electrospun scaffold for nerve tissue engineering applications, Mater. Technol. 35 (2020) 92–101.

[31] Z. Mohammadalizadeh, E. Bahremandi-Toloue, S. Karbasi, Synthetic-based blended electrospun scaffolds in tissue engineering applications, J. Mater. Sci. 57 (2022) 4020–4079.

[32] C.Y. Lin, S.C. Luo, J.S. Yu, T.C. Chen, W.F. Su, Peptide-based polyelectrolyte promotes directional and long neurite outgrowth, ACS Appl. Bio Mater. 2 (2019) 518–526.

[33] T.L. Ma, S.C. Yang, T. Cheng, M.Y. Chen, J.H. Wu, S.L. Liao, W.L. Chen, W.F. Su, Exploration of biomimetic poly(γ-benzyl-L-glutamate) fibrous scaffolds for corneal nerve regeneration, J. Mater. Chem. B 10 (2022) 6372–6379.

[34] Z.H. Wang, Y.Y. Chang, J.G. Wu, C.Y. Lin, H.L. An, S.C. Luo, T.K. Tang, W.F. Su, Novel 3D neuron regeneration scaffolds based on synthetic polypeptide containing neuron cue, Macromol. Biosci. 18 (2018) 1700251.

[35] K. Hashimoto, T. Ishima, A novel target of action of minocycline in NGF-induced neurite outgrowth in PC12 cells: translation initiation factor eIF4AI, PLoS One 5 (2010) e15430.

[36] A. Kuroda, T. Fuchigami, S. Fuke, N. Koyama, K. Ikenaka, S. Hitoshi, Minocycline directly enhances the self-renewal of adult neural precursor cells, Neurochem. Res. 43 (2018) 219–226.

[37] T. Tao, J.Z. Feng, G.H. Xu, J. Fu, X.G. Li, X.Y. Qin, Minocycline promotes neurite outgrowth of PC12 cells exposed to oxygen-glucose deprivation and reoxygenation through regulation of MLCP/MLC signaling pathways, Cell, Mol. Neurobiol. 37 (2017) 417–426.

[38] A.J.A. Su, N. Jiang, S.C. Luo, K.M. Washington, M.C. Wu, Y.C. Huang, W.F. Su, Fibrous polypeptide based bioscaffold delivery of minocycline hydrochloride for nerve regeneration, Mater. Chem. Phys. 305 (2023) 127974.